Sequence-Dependent Dynamics in Duplex DNA

T. M. Okonogi,* S. C. Alley,*† A. W. Reese,* P. B. Hopkins,* and B. H. Robinson*
*Department of Chemistry University of Washington, Seattle, Washington 98195-1700, and †Department of Chemistry, The Pennsylvania State University, University Park, Pennsylvania 16802 USA

ABSTRACT The submicrosecond bending dynamics of duplex DNA were measured at a single site, using a site-specific electron paramagnetic resonance active spin probe. The observed dynamics are interpreted in terms of the mean squared amplitude of bending relative to the end-to-end vector defined by the weakly bending rod model. The bending dynamics monitored at the single site varied when the length and position of a repeated AT sequence, distant from the spin probe, were changed. As the distance between the probe and the AT sequence was increased, the mean squared amplitude of bending seen by the probe due to that sequence decreased. A model for the sequence-dependent internal flexural motion of duplex DNA, which casts the mean squared bending amplitudes in terms of sequence-dependent bending parameters, has been developed. The best fit of the data to the model occurs when the $(AT)_n$ basepairs are assumed to be 20% more flexible than the average of the basepairs within the control sequence. These findings provide a quantitative basis for interpreting the kinetics of biological processes that depend on duplex DNA flexibility, such as protein recognition and chromatin packaging.

INTRODUCTION

The flexibility of duplex DNA is important for its functionality, particularly in the areas of protein-DNA binding (Hogan and Austin, 1987), interactions with architectural transcription proteins (Wolffe, 1994; Grove et al., 1996a; Nardulli et al., 1996), packaging DNA into chromatin (Richmond et al., 1984; Patikoglou and Burley, 1997; Hagerman, 1988), strand exchange (Thompson et al., 1976), and deletion formation (Chedin et al., 1994). In 1988, Hagerman (1988) concluded that little convincing evidence existed in favor of the hypothesis that DNA flexibility is sequence dependent. In 1994, Harrington and Winicov (1994) extensively reviewed the interactions between DNA and a number of proteins in which "the relatively new concept of sequence-directed structural softness or flexibility" is implicated as a physical basis for DNA-protein recognition.

Until now, there have been no experiments quantitatively evaluating the sequence-dependent flexibility in duplex DNA. A number of specific sequences have been suggested as more flexible; in particular, the dinucleotide CA and TA steps have been suggested as candidates for regions of increased flexibility based on the results of gel mobility assays (Harrington and Winicov, 1994). Harrington suggests that sequence-dependent flexibility may account for unexplained differences in the gel mobilities between GGGCCC motifs and AAAAAA tracts in cyclization assays (Dlakic and Harrington, 1995). In the formation of chromatin structures, long runs of homopolymers (dA)-(dT) and (dG)-(dC) are excluded from the DNA-histone packaging, presumably because of rigidity (Drew and Travers, 1985), while sequences containing AAA, AAT, and TA repeats bind well (Patikoglou and Burley, 1997). Hogan and Austin examined bacteriophage 434 repressor binding affinity for DNA sequences (Hogan and Austin, 1987) and concluded that protein binding correlated with the basepair sequence central to the operator binding sites. It was suggested that binding was proportional to a sequence's ability to twist or flex and that the observed variation in DNA stiffness was sequence dependent.

When there is a change in the dynamics due to a particular change in sequence in duplex DNA, it occurs for one of two reasons. The first could be a global change in the set of secondary structures induced by a specific sequence. An example of this was presented by Schurr and co-workers, who studied the effect of a 16-bp $(CG)_8$ insert in a linear 1.1-kbp duplex DNA sequence. Their data implied that the insert induced a large change in secondary structure throughout the molecule (Kim et al., 1993). The second reason for a change in dynamics is that a sequence has a locally different flexibility, which in the context of a large section of DNA may affect the dynamics of other bases through the internal collective modes. An example of a local change in flexibility affecting dynamics or kinetics elsewhere in the DNA is the process by which inserts are deleted between directing 18-bp repeats flanking the deletion segment (Chedin et al., 1994).

In general, if an effect is local but is communicated via the DNA to other parts, then the effect should be characterized by a fall-off with distance. Fall-off of an effect with distance is a characteristic of structural alterations or allosterism. It is also a characteristic of internal dynamic twisting correlations (Schurr and Fujimoto, manuscript submitted for publication) and internal dynamic bending correlations, as will be shown later. One example of such a fall-off that was interpreted in terms of allosterism is that of the effect of a $(CG)_4$ insert on the rate of cleavage by restriction enzymes at specific sites. The state of the $(CG)_4$ insert was controlled

Received for publication 9 September 1999 and in final form 17 January 2000.

Address reprint requests to Dr. Bruce H. Robinson, Department of Chemistry, University of Washington, Box 351700, Seattle, WA 98195. Tel.: 206-543-1773; Fax: 206-685-8665; E-mail: robinson@chem.washington.edu.

0006-3495/00/05/2560/12 $2.00

by the presence of $[Co(NH_3)_6]^{3+}$ and, presumably, varied locally between B- and Z-form DNA. When the insert adopted an alternative right-handed structure, a severalfold enhancement in the cutting rate was observed for sites up to 50 bp from the cutting site. Even in the absence of $[Co(NH_3)_6]^{3+}$, an enhancement in the cutting rate was observed when the insert was placed up to 50 bp from the cutting site in linear DNA (Aloyo et al., 1993; Schurr et al., 1997a; Ramsauer et al., 1997). The above example illustrates how long-range structural correlations can propagate over a finite domain and die off with distance.

In this paper we will show that the observed changes in flexibility seen by an electron paramagnetic resonance (EPR) active probe are quantitatively well explained by a modified weakly bending rod model. This model supports the ideas that 1) increased motion may be due to a local change in the flexibility of the DNA molecule and 2) certain sequences of DNA may have different propensities for bending. Examples of the consequences of local changes in flexibility for structure or function will be discussed.

We have previously investigated DNA dynamics by EPR, using a nitroxide rigidly fused to a pyrimidine base, **Q**, paired to 2-aminopurine (2AP) (Fig. 1) (Miller et al., 1995; Okonogi et al., 1999). It was shown that the Q-2AP basepair reports the dynamics of the attached DNA and that the probe motion independent of the attached DNA was small relative to the motion induced by the DNA. In particular, this probe is primarily sensitive to bending dynamics and thus provides an excellent method for quantitatively determining the flexibility of DNA. In the following experiments, the probe is used in a site-specific manner by being placed in a small region of duplex DNA whose sequence is kept fixed. The DNA is linear, relaxed, and nonstressed. At well-defined distances from the probe, there is a test region in which the basepair sequence is varied. The effect of the test region on the dynamics of the site-specific probe is interpreted as differences in the coupling of basepairs to one another. The sources of the dynamics include 1) the overall tumbling of the DNA, 2) the internal collective modes of motion, and 3) the motion of the probe (including the basepair) independent of the macromolecular environment. To test the effects of the collective modes of motion on the probe, the following experiments were designed so that 1) an 11-bp region containing the probe and 2) the overall length of the DNA remain constant throughout the experiments. These two constraints on the DNA ensure that the overall tumbling and the length-independent motions of the probe are constant among the experiments. The internal collective modes provide the only mechanism for motions in one region of the DNA to affect the probe. Preliminary results on the sequence-specific bending of duplex DNA, obtained with a site-specific probe, have previously been reported (Okonogi et al., 1997, 1998, 1999).

The present measurements pertain to the dynamic bending rigidity that governs the submicrosecond flexural dynamics of DNA. Its corresponding dynamic persistence length is P_{db} = 1500–2000 Å (Okonogi et al., 1999; Naimushin et al., 2000), and because of its considerable stiffness, it partially contributes to the equilibrium mean squared bending between basepairs, to the effective equilibrium bending rigidity of DNA and to P_{tot}. As discussed elsewhere (Schurr et al., 1997a,b; Okonogi et al., 1999; Naimushin et al., 2000), P_{tot} apparently contains contributions not only from dynamic bends and sequence-dependent permanent bends, but also from slowly relaxing bends that arise from fluctuations between distinct secondary conformations with different intrinsic curvatures. Consequently, the bending rigidity is time-dependent, relaxing from its initially stiff value characteristic of P_{db} = 1500–2000 Å to a value about half as great at long times. By themselves, the present experiments provide no information about the variation of this slowly relaxing contribution to mean squared bending with DNA sequence. Thus any slowly relaxing contributions to the equilibrium bending rigidity conceivably might behave differently.

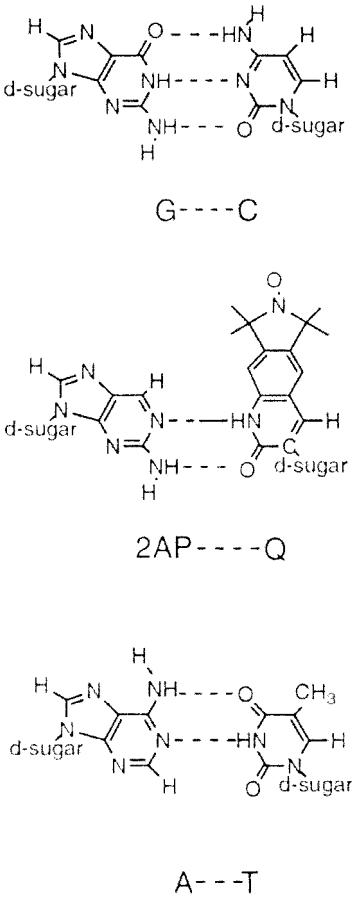

FIGURE 1 Basepairs G-C, 2AP-**Q**, and A-T. 2-Aminopurine (2AP)-**Q** is a modified adenosine-thymidine basepair. The guanosine-cytosine and adenosine-thymidine basepairs are shown for comparison.

A MODIFIED WEAKLY BENDING ROD THEORY

To investigate the sequence dependence of DNA flexibility, we extend the theory developed by Schurr and co-workers for the elastic motion of the bending of duplex DNA (Wu et al., 1987; Song and Schurr, 1990; Schurr et al., 1991; Okonogi et al., 1999). The weakly bending rod theory assumes that the DNA is stiff enough that the twisting modes of motion are uncoupled from those of bending. The DNA is assumed to behave like a flexible rod that has mean local cylindrical symmetry. The uniform rotational modes of motion are 1) rotation about the cylinder axis (the z direction) and 2) rotation about the x and y axes. Each basepair is coupled to its neighbors by a harmonic bending potential, which generates a torque to each basepair and thereby governs the extent of angular rotations due to bending. The internal potential is a quadratic function of the differences between the angular displacements of successive bond vectors from the end-to-end vector. The force constant between basepairs, κ, is taken to be the same for rotation about x and y, where η and θ are the angles of rotation about x and y, respectively. For the case where the force constants between basepairs, κ, are independent of DNA composition, the internal potential is

$$U = \tfrac{1}{2}\kappa \sum_{i=1}^{N}(\eta_{i+1} - \eta_i)^2 + \tfrac{1}{2}\kappa \sum_{i=1}^{N}(\theta_{i+1} - \theta_i)^2 \qquad (1)$$

This can be recast into a matrix form:

$$U = \tfrac{1}{2}\kappa\vec{\eta}^{t}\mathbf{A}\vec{\eta} + \tfrac{1}{2}\kappa\vec{\theta}^{t}\mathbf{A}\vec{\theta} \qquad (2)$$

The $\mathbf{A}$ matrix is a second-order finite-difference matrix. Explicitly, for the example of 4 bp, $\mathbf{A}$ is

$$\mathbf{A} = \begin{pmatrix} 1 & -1 & 0 & 0 \\ -1 & 2 & -1 & 0 \\ 0 & -1 & 2 & -1 \\ 0 & 0 & -1 & 1 \end{pmatrix} \quad \text{and} \quad \vec{\eta} = \begin{pmatrix} \eta_1 \\ \eta_2 \\ \eta_3 \\ \eta_4 \end{pmatrix}$$

The mean squared amplitudes of internal bending can be found from this potential (Wu et al., 1987; Song and Schurr, 1990):

$$\langle\vec{\eta}(\infty)\vec{\eta}^{t}(\infty)\rangle = \frac{\int_{-\infty}^{\infty}\vec{\eta}\exp^{-(U/kT)}\vec{\eta}^{t}\,d\eta^{N}}{\int_{-\infty}^{\infty}\exp^{-(U/kT)}d\eta^{N}} = \frac{kT}{\kappa}\mathbf{Q}\Lambda^{-1}\mathbf{Q}^{t} \qquad (3)$$

where k is Boltzmann's constant, T is the absolute temperature, $d\eta^{N} = d\eta_1 d\eta_2 d\eta_3 \ldots d\eta_N$, and $\mathbf{Q}$ is the transformation matrix that diagonalizes $\mathbf{A}$. The matrix $\mathbf{Q}\Lambda^{-1}\mathbf{Q}^{t} = \mathbf{A}^{-1}$ is the pseudoinverse of $\mathbf{A}$. Λ is the diagonal matrix that contains the eigenvalues of $\mathbf{A}$. The uniform sheer mode eigenvalue of $\mathbf{A}$ is zero and is removed from the inverse, as it is not one of the internal bending modes. The total mean squared amplitude of bending, $\langle\beta_i^2(\infty)\rangle$, is the sum of the two bending contributions plus a length-independent contribution, $\langle\beta_o^2(\infty)\rangle$, to the basepair at the ith position:

$$\langle\beta_i(\infty)\beta_i(\infty)\rangle = \langle\beta_o(\infty)\beta_o(\infty)\rangle + \langle\eta_i(\infty)\eta_i(\infty)\rangle + \langle\theta_i(\infty)\theta_i(\infty)\rangle$$

or more simply,

$$\langle\beta_i^2(\infty)\rangle = \langle\beta_o^2(\infty)\rangle + 2\langle\eta_i^2(\infty)\rangle \qquad (4)$$

As has been shown elsewhere (Hustedt et al., 1993; Allison et al., 1982),

$$\langle\beta_i^2(\infty)\rangle = \frac{kT}{\kappa}\frac{(N+1)}{6}\cdot\left\{1 + 3\left(\frac{2i - (N+2)}{N+1}\right)^2\right\} + \langle\beta_o^2(\infty)\rangle$$

The mean squared amplitudes increase nearly in proportion to the length of the DNA. The mean squared amplitude of motion is the quantity that is obtained from the experiments. This may be compared to a related quantity: the mean squared difference amplitude. This quantity is found from the orientation difference $\Delta\beta_i = \beta_{i+1} - \beta_i$, from which it follows that $\langle\Delta\beta_i^2(\infty)\rangle = 2(kT/\kappa)$, by Eqs. 3 and 4. This quantity describes the extent of bending relative to the neighboring bases. The extent of bending of the difference amplitude is independent of DNA length and of position in the duplex. This may be contrasted with the total amount of bending, $\langle\beta_i^2(\infty)\rangle$, reported by the probe, which increases in proportion to the length. This is an important distinction, which will become useful shortly.

We now extend the weakly bending rod theory to consider the possibility of different force constants between different basepairs along the DNA molecule. In principle, each nearest-neighbor basepair interaction can have its own force constant. The bending force constants are still nearest neighbor and the potential energy has only nearest-neighbor interactions, but the value of the force constants may depend upon sequences that may include many basepairs in the immediate vicinity. Let $\bar{\kappa}$ represent the mean force constant ($\bar{\kappa} = ((1/N)\sum_{j=1}^{N}\kappa_j)$), and let r_j be the ratio of $\kappa_j/\bar{\kappa}$. Then Eq. 2 can be written in the same form, as originally developed, and κ can be replaced by $\bar{\kappa}$. The $\mathbf{A}$ matrix is not as simple as given in Eq. 3. Now the potential matrix, $\mathbf{A}$, is written in terms of the ratios of force constants. For the example of 4 bp,

$$\mathbf{A} = \begin{pmatrix} r_1 & -r_1 & & \\ -r_1 & r_1 + r_2 & -r_2 & \\ & -r_2 & r_2 + r_3 & -r_3 \\ & & -r_3 & r_3 \end{pmatrix} \quad \text{where } r_j = \frac{\kappa_j}{\bar{\kappa}} \qquad (5)$$

At present, we make some simplifying assumptions in the model. Rather than develop a set of force constants unique to each dinucleotide pair from 5′ to 3′, we have chosen to assume that $\kappa(\text{AT}) = \kappa(\text{TA})$ and that all force constants outside the region of the test sequence are the average value. In future papers, we will explore more elaborate models. For now the model admits nonunity force constant ratios between the A-to-T basepairs only in the region of the test

sequence, while the control sequence of basepairs flanking the variable test sequences is controlled by a mean force constant, $\bar{\kappa}$. The matrix in Eq. 5 is used in the following way. The force constants between basepairs in the sample molecule outside of the test sequence are set to a mean value, $\bar{\kappa}$, or $r_j = 1$ in this region. A test sequence insert can have a set of ratios, r_j, that depend on the details of the sequence. For the test sequence inserts presented here we will assume that there is only a single force constant between basepairs, κ', which is different from the mean. Then $r = \kappa'/\bar{\kappa}$ is the single ratio that describes the test sequence as having different forces between basepairs. r will be less than 1 for sequences that are more flexible than the average and greater than 1 for sequences more rigid than average. In general,

$$\langle \beta_i^2(\infty)\rangle = 2\frac{kT}{\bar{\kappa}}(\mathbf{A}^{-1})_{ii} + \langle \beta_o^2(\infty)\rangle \tag{6}$$

In nearly all cases, the probe is placed at position $i = 6$ in the DNA. The experiment monitors the mean squared amplitude of motion, $\langle \beta_6^2(\infty)\rangle$, due to the collective modes seen by the probe at position 6. There are $N + 1$ basepairs, of which L are distinct in the sense that $r \neq 1$, and they range from position N_1 to N_2. The length of the distinct test sequence is $L = N_2 - N_1 + 1$. There is a single distinct force constant ratio, r, for the L distinct basepairs in the test sequence. For this simple model, we can vary the length of the DNA, $N + 1$; the length of the insert, L; the starting position, N_1; and the force constant ratio, r. The matrix $\mathbf{A}$ is a function of $N + 1$, L, N_1, and r. As an example, for the case where $L = 3$, $N_1 = 3$, and $N + 1 = 8$,

$$\mathbf{A}(r) = \begin{pmatrix} 1 & -1 & & & & & & \\ -1 & 2 & -1 & & & & & \\ & -1 & 1+r & -r & & & & \\ & & -r & 2r & -r & & & \\ & & & -r & 1+r & -1 & & \\ & & & & -1 & 2 & -1 & \\ & & & & & -1 & 2 & -1 \\ & & & & & & -1 & 1 \end{pmatrix} \tag{7}$$

The mean squared amplitudes are explicitly a function of r, $\langle \beta_i^2(\infty)\rangle(r) = \langle \beta_i^2(\infty)\rangle$. With this simple model, we can explore the effects of sequence variation at a site distant from the probe. Sequence variation is modeled by different values of the bending constant ratio, r. When $r = 1$, there is no difference in dynamics between the test and control sequences and no dependence on the length of the test sequence or its distance from the probe. The DNA outside of the test sequence insert region will always have $r = 1$ and for our purposes here will be referred to as "average" DNA. When $r \neq 1$ in the test sequence region, we measure that change in flexibility as the difference in flexibility due to the difference between r and 1:

$$\Delta_r\langle \beta_6^2(\infty)\rangle = \langle \beta_6^2(\infty)\rangle(r \neq 1) - \langle \beta_6^2(\infty)\rangle(r = 1)$$

In Fig. 2, the theoretical difference bending amplitude $\Delta_r\langle \beta_6^2\rangle$ is shown as a function of r, the ratio of force constants, for various lengths of test sequences and lengths of DNA. All test sequences started at position $N_1 = 7$, and the difference mean squared bending amplitude was calculated at position 6. The difference mean squared amplitude is nearly linear with the inverse ratio of the force constants, r, and is nearly proportional to the length of the test sequence, L. From Eq. 5, if all bases are of flexibility $r\bar{\kappa}$, then $A(r) = rA(1)$. In this limit then, $\Delta_r\langle \eta_{ii}^2\rangle \propto (1/r - 1)A_{ii}(1)$. We find that the following empirical functional form (Eq. 8) satisfactorily simulated the computations using Eq. 6 and matrices of the form of Eq. 7. For the case where $i = 6$ and $N_1 = 7$,

$$\Delta_r\langle \beta_6^2(\infty)\rangle \approx -2 \cdot \frac{k_B T}{\bar{\kappa}} \cdot L \cdot \left(\frac{r-1}{r}\right) \cdot \{1 - \exp^{-((N-L)/N_0)^{1/2}}\} \tag{8}$$

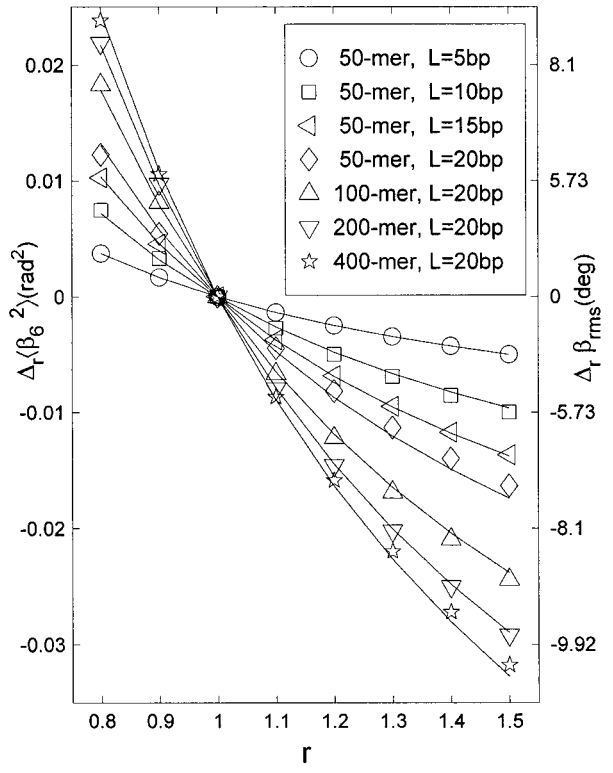

FIGURE 2 Mean squared bending amplitudes, $\Delta_r\langle \beta_6^2\rangle$ (rad^2), and rms angular displacements, β_{rms} (deg), are shown as a function of the force constant ratio, r, for DNAs of length $N + 1 = 50$, and test sequences of lengths $L = 5$ (○), 10 (□), 15 (◁), and 20 (◇), and for DNAs with test sequence lengths $L = 20$ and $N + 1 = 50$ (◇), 100 (△), 200 (▽), and 400 (☆) basepairs. All sequences begin at position $N_1 = 7$, and the mean squared bending amplitude is measured at position 6. $k_BT/\bar{\kappa} = 0.00272$ rad^2, a typical value (Okonogi et al., 1999). $N_0 = 70$ bp. Estimates of $\Delta_r\langle \beta_6^2\rangle$ values from Eq. 8 are plotted as lines and compared with the exact calculations (shown as *icons*).

N_o is the length of the DNA at which $\Delta_r\langle\beta_6^2\rangle$ becomes independent of N and demonstrates that there is a limit to the amount of DNA that can be added to enhance the difference effect due to an insert of length, L, and ratio, r. Fig. 2 compares this analytic form (Eq. 8) with the exact results. The difference mean squared amplitude, $\Delta_r\langle\beta_i^2\rangle$, depends approximately exponentially on the ratio of the length of the DNA to N_o.

Fig. 3 demonstrates theoretically the effect that an insert with force constant ratio r can have on the internal amplitudes of bending seen by a nearby probe. $\Delta_r\langle\beta_i^2\rangle$ is plotted as a function of the total length of the DNA for a fixed insert and a fixed distance between the insert and the probe. Initially there is a 20-mer DNA with the probe, **Q**, at position 6, $N_1 = 11$ and $N_2 = 20$, and the test insert has force constant ratio, r. $L = 10$ bp is the length of the test sequence insert. The extend left curve (*triangles pointing left*) extends the initial 20-mer to the left of the initial DNA with a region of average DNA ($r = 1$ in this region). Notice that the difference drops off to nearly zero at ~200 bp. The extend right curve (*triangles pointing right*) extends the original 20-mer to the right side of the test sequence, so that the test sequence is between the added average DNA and the probe. The difference increases with increasing length of DNA and becomes independent of DNA length at ~400 bp. For the case where the DNA is extended in both directions, the curve (*diamonds*) demonstrates that the effect is an average of the effects due to the extension to the left and to the right. Empirical functional forms, which satisfactorily model the computations, are given in the legend and are shown as solid lines in Fig. 2.

These calculations provide insight into how the experiments should be designed to best detect the effect of an insert with a different inherent flexibility. The test insert should be located between the spin probe and a long region of average DNA. The region of average DNA enhances the difference in bending amplitudes observed by the probe up to about $N_o = 70$ bp; beyond that the increase in the difference is negligible. Notice that the probe's mean squared amplitude of motion increases without bound, but the difference in amplitudes due to the test sequence becomes a constant value as the length of DNA goes to infinity. It is interesting to note that, when the test region is between the probe and the average DNA, the presence of average DNA is beneficial in amplifying, and never overshadows, the motional effect of the test sequence on the probe. In contrast, when the probe is between the average DNA and the test insert, the average region can overshadow the effect of the test sequence.

We now consider how a sequence will affect the internal motion, when that sequence is moved further away from the probe, which is part of the base where the bending amplitudes are being monitored. In Fig. 4, the mean squared amplitude is shown as a function of the test sequence's starting position, N_1, for representative lengths, L, and ratios, r, when N is held constant. According to the theory, the initial amplitudes, $A_o(r; N, L)$, are dependent upon N, r, and L. The mean squared amplitude, seen at position 6, evolves

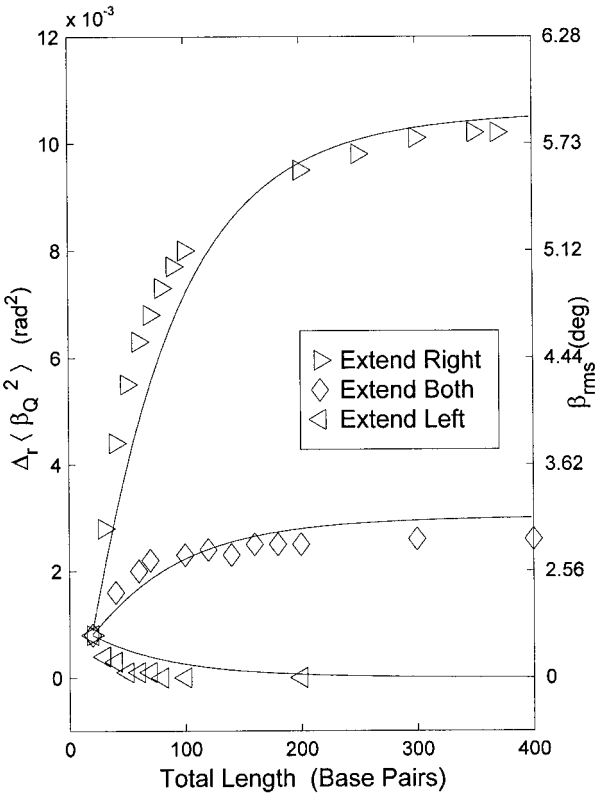

FIGURE 3 Plots of the difference in the mean squared amplitudes of bending as a function of **Q** (probe) and L (test sequence) placement in three uniquely growing chains of DNA for $r = 1$ and $r = 0.815$. Every curve begins with a 20-mer DNA with **Q** at position $i = 6$, $N_1 = 11$, and $N_2 = 20$, where $L = 10$ bp in length. The extend right curve (▷) extends the original 20-mer towards the 3′ end away from **Q** and L. The extend left curve (◁) extends the initial 20-mer to the left, or 5′ of **Q**. The extend both curve (◇) extends the initial 20-mer on both ends of the DNA simultaneously and appears as a linear combination of the right and left, as seen in the fitting formulas:

Extend Left

$$\Delta_r\langle\beta_i^2(\infty)\rangle \approx -2\cdot\frac{k_BT}{\bar{\kappa}}\cdot\left(\frac{r-1}{r}\right)\cdot L\cdot 0.14\cdot\exp(-(N-L)/N_o]\cdot\exp[-4/\langle N\rangle]$$

Extend Right

$$\Delta_r\langle\beta_i^2(\infty)\rangle \approx -2\cdot\frac{k_BT}{\bar{\kappa}}\cdot\left(\frac{r-1}{r}\right)\cdot L\cdot 0.9\cdot\{1-\exp[-(N-L/N_o)]\}\cdot\exp[-4/\langle N\rangle]$$

The equation for extending in both directions simultaneously is an average of the left and right equations, using 30% of the extend right curve and 70% of the extend left curve. All three curves depend exponentially on the length of the DNA, with a characteristic relaxation length of $N_o = 70$ bp and $\langle N\rangle = (N-2)/2$.

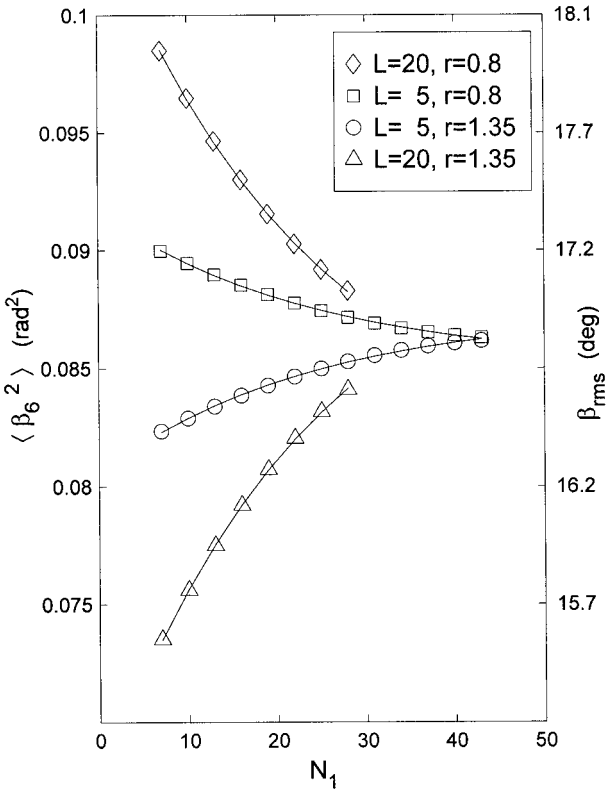

FIGURE 4 Plots of the mean squared amplitude of bending and rms angular displacements as a function of the starting position N_1 for $L = 5$ and 20 bp and $r = 0.8$ and 1.35 for DNAs of length $N + 1 = 50$ bp for $L = 20$, $r = 0.8$ (◇); $L = 5$, $r = 0.8$ (□); $L = 5$, $r = 1.35$ (○); and $L = 20$, $r = 1.35$ (△). Data are fit to single-exponential functions of N_1 (Eq. 9).

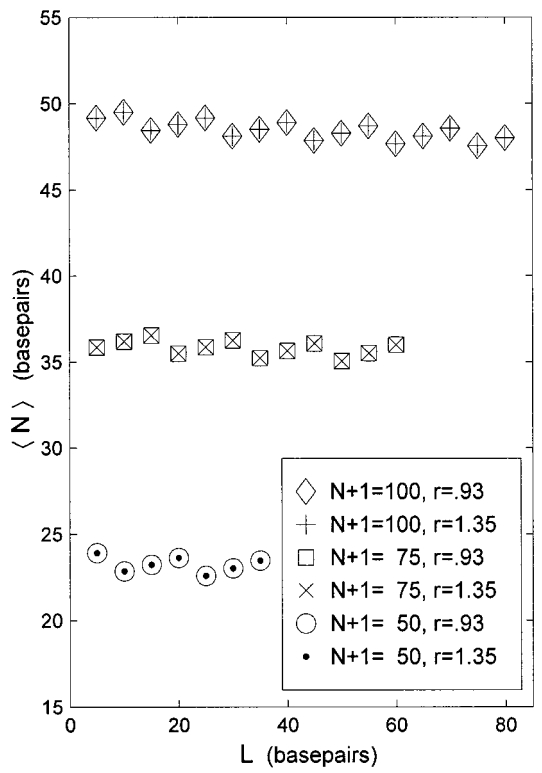

FIGURE 5 Correlation length $\langle N \rangle$ for different test sequence lengths L, force constant ratios r, and DNA lengths $N + 1$ obtained from fits to calculations similar to those shown in Fig. 4. $\langle N \rangle$ are calculated for $N + 1 = 100$ when $r = 0.93$ (◇) and $r = 1.35$ (+), $N + 1 = 75$ when $r = 0.93$ (□) and $r = 1.35$ (×), and $N + 1 = 50$ when $r = 0.93$ (○) and $r = 1.35$ (●). Mean correlation values $\langle\langle N \rangle\rangle$ and standard deviations:

$N + 1$	$r = 0.93$	$r = 1.35$	$\langle\langle N \rangle\rangle$	$(N - 2)/2$
50	○	●	23.2 ± 0.5	23.5
75	□	×	35.8 ± 0.5	36.0
100	◇	+	48.5 ± 0.6	48.5

All values were measured at position 6, the position of the probe. Sequences began at $N_1 = 7$ and went as far as logically possible to satisfy $N_{1\max} + L < N + 1$.

toward the average value of the $N + 1$-mer (where all $r = 1$, as given, for example, by the NT sequence) as N_1 increases to the length of the molecule ($N_1 = N + 1$). The rate at which the effect of the test sequence falls off, however, is independent of r and L. This remarkable result was not obvious from the model and simplifies our interpretation of the effect of an insert on the motion seen at the probe. To demonstrate the effect of increased N_1 at constant N, overlaid on the mean squared amplitudes in Fig. 4 is an exponential function of the form

$$\langle \beta_6^2(\infty) \rangle = A_o(r; N, L) * \exp^{-(N_1-7)/\langle N \rangle} + B_o(r; N, L) \qquad (9)$$

where $A_o(r; N, L)$ and $B_o(r; N, L)$ are the least-squares optimized fitting parameters. $\langle N \rangle$ is the correlation length in basepairs and represents the extent to which the mean squared amplitude is affected by that insert. The overlay of a single exponential, in Fig. 4, shows that this model function is a satisfactory approximation to the dependence of the mean squared amplitude on N_1.

Fig. 5 plots the correlation length, $\langle N \rangle$, for different L, r, and $N + 1$. The astoundingly simple result is that the correlation length is always approximately half the total number of basepairs: $\langle N \rangle \cong (N - 2)/2$. $\langle N \rangle$ is independent of L, r, and $\bar{\kappa}$. Lengths of DNA up to $N + 1 = 200$ were tested for $\langle N \rangle$ (not shown in Fig. 5). This effect can be qualitatively understood in the following way. We note first that the alteration of the bending potential in one region of the molecule has no effect whatsoever on the equilibrium distribution of bending angles between successive bond vectors, $\langle \Delta\beta_i^2(\infty) \rangle$, or on the mean squared curvature, at any other point in the molecule. It is important to note that the mean squared angular displacements under discussion, namely $\langle \beta_i^2(\infty) \rangle$, are those of a given bond vector with respect to the end-to-end vector of the entire filament. When viewed from the local frame of the probe, the effect of increasing the flexibility of some distal region is to increase the mean squared angular displacement of the end-to-end vector away from the bond vector of the probe. The end-to-end vector is a normalized sum of all of the bond vectors

between neighboring bases in the DNA molecule. In the frame of the probe, all bond vectors from the end containing the probe up to the site of increased flexibility remain unchanged, and beyond the flexible region all bond vectors are rotated upon flexing. By placing the region of flexibility as close to the probe as possible, the maximum number of bond vectors are rotated, and the largest displacement of the end-to-end vector relative to the probe bond vector occurs. As the flexible region is moved away from the probe, flexing will rotate fewer bond vectors, and the effect falls away.

CONCLUSIONS FROM THEORY

The overall impact of a test sequence on the motion of the probe falls off exponentially with the increasing length of an intervening average sequence, when the total length of the DNA is kept fixed. The correlation length over which the dynamical communication is maintained depends only on the total length of the duplex DNA and is $\frac{1}{2}(N + 1)$. Differences in the bending dynamics seen by the probe due to a test sequence are enhanced by adding more average DNA. The difference in the internal bending, $\Delta_r\langle\beta_i^2\rangle$, for an average sequence (for instance, NT) and for one that is more flexible (like that of an $(AT)_n$ sequence) increases exponentially with increasing length of the molecule up to ~70 bp, and this length is different from $\frac{1}{2}(N + 1)$.

The result, $\langle N\rangle \cong (N - 2)/2$, is valid within the context of the weakly bending rod model. However, there must be a point at which the correlation length, $\langle N\rangle$, is cut off by the total persistence length of the DNA, beyond which angular correlations are lost in any case. That is, when the contour length exceeds the persistence length, then the correlation length must be limited by the persistence length. One can express this idea mathematically by assuming a form similar to that suggested for the addition of persistence lengths (Schellman and Harvey, 1995):

$$\frac{1}{\langle N\rangle} = \frac{2}{N-2} + \frac{2h}{P_{tot}}. \qquad (10)$$

EXPERIMENTAL METHODS

A series of duplex DNAs were constructed, all of which were 50 bp in length. The spin probe base, **Q** (Fig. 1), is always at position 6 in the initial 11-bp sequence, and the test sequences never begin before position 12. The control sequence (NT) is basepairs 1087 to 1136 from *Drosophila melanogaster* TATA-box binding protein TFIID gene:

5′d[CCT CGQ ATC GTG CTC CTC ATC TTC

GTG TCC GGA AAG GTG GTG CGC ACT GG]

The constructs that were tested contained the dinucleotide repeat $(AT)_n$. $(AT)_n$ inserts were chosen because they lack retarded polyacrylamide gel electrophoretic mobilities, indicating that these sequences do not contain permanent bends (Hagerman, 1990); because $(AT)_n$ sequences are thought to be very flexible (Harrington and Winicov, 1994); and because $(AT)_n$ sequences have not been implicated in inducing allosteric transitions. The test sequence names describing the insert composition, test sequence length L, test sequence base starting position N_1, and stopping position N_2, all with **Q** at position 6, are listed in Table 1. For example, the sequence listed AT4 is

5′d[CCT CGQ ATC GTA TAT ATA

TTC TTC GTG TCC GGA AA

G GTG GTG CGC ACT GG]

where the unbolded sequence is the test sequence.

In addition to the poly-$(AT)_n$ basepair test sequences, we inserted a dipropylene linker moiety, DPL (5′O-$(CH_2)_3$O-PO_2^--O-$(CH_2)_3$O-3′), into the NT control sequence. DPL is close in size to 2 bp, but is missing the sugar and base. This linker is placed in both strands of the duplex DNA in a complementary fashion but does not replace any of the 50 basepairs. Such a linker was designed with the intention of showing the extent to which EPR spectra are sensitive to very weak coupling between the two segments, which are the 11-mer sequence containing the dynamics probe and the remaining 39-mer sequence in the molecule. Furthermore, the DPL sample demonstrates the extent to which the dynamics of the two segments of the DNA can be fully decoupled.

Q was prepared as previously described (Miller et al., 1995), using both the naturally abundant [$^{14}N,H_{12}$] and the isotopically substituted [$^{15}N,D_{12}$] nitroxides. **Q** was site-specifically attached at the sixth position of every 50-mer duplex DNA sampled. The duplexes were prepared using the Klenow polymerase filling technique (Maniatis et al., 1989). All oligomers were synthesized on an ABS 6800 or 392 DNA synthesizer and purified using reverse-phase (trityl-on purification) high-performance liquid chromatography on a Dynamax 300-Å column. 0.4 OD of the 11-mer primer strand containing **Q** at the sixth position (DNA 5′-d(CCT CG**Q** ATC GT)) was annealed with 2.0 OD of the appropriate template 50-mer and combined with 10 mM each of dATP, dCTP, dGTP, and dTTP, and 50 units of Klenow fragment or 20 units of Vent polymerase in 1× primer extension buffer or ThermoPol buffer. After incubation, the reaction mixture was purified by nondenaturing polyacrylamide gel electrophoresis. DNA was extracted from the gel, using the crush-and-soak procedure (Maniatis et al., 1989) in duplex elution buffer. Extracted DNA was ethanol precipitated, dried, and resuspended in 10 μl PNE buffer (10 mM phosphate (pH 7.0), 0.1 mM EDTA, and 100 mM NaCl).

CW-EPR spectra were digitally recorded on a spectrometer with a loop gap resonator cavity (Mailer et al., 1991) and a commercial Bruker EMX spectrometer with a TE102 cavity. Parameters employed for CW-EPR measurements include a 10-kHz modulation frequency, 1.0-G modulation

TABLE 1 The names of the sequences made with the probe, Q, at position 6, and the length of the test sequence, *L*, and the start, N_1, and stop, N_2, positions of the test sequence

Sequence name	L	N_1	N_2
NT	0	—	—
DPL	2	12	12
AT4	8	12	19
AT10	20	12	31
AT15	30	12	41
AT7A	15	12	26
AT7As5	15	17	31
AT7As12	15	24	38
AT7As24	15	36	50

All sequences are, in total, 50 bp in length. $N_1 = N_2$ for DPL because the linker separates basepairs 11 and 12, acting as a universal swivel joint.

amplitude, 0.1 mW power, 1024 points, and 30°C regulated to ±0.2°C, well below T_m for these molecules (Okonogi et al., 1999). Line samples of 1–2 OD (100–200 μM) duplex DNA were placed in either a 0.6 × 0.84 mm or 0.8 × 1.0 mm quartz capillary and stored at 4°C between EPR measurements. Known rigid limit **A** and **g** tensors were obtained elsewhere (Reese, 1996), and the uniform mode correlation times were used to simulate the spectra of the B-form 50-mers in PNE solution at 30°C. The change in spectral width arises from a rapid dynamics averaging of the **A** tensor elements. The observed spectral width is proportional to the dynamically averaged tensor element, $\langle A_{zz}\rangle$, which is directly related to the order parameter, S_6, and to the mean squared internal oscillation amplitude, $\langle\beta_6^2(\infty)\rangle$, by the relation

$$S_i = \frac{\langle Azz\rangle - \bar{a}}{Azz - \bar{a}} = \frac{3\langle\cos^2\theta\rangle - 1}{2}$$

$$= \frac{3\exp\{-2\langle\beta_i^2\rangle\} + 1}{4} \approx 1 - \frac{3}{2}\langle\beta_i^2\rangle \qquad (11)$$

where $\bar{a} = \frac{1}{3}trA$ and is independent of probe motion (Hustedt et al., 1993).

$\langle\beta_6^2(\infty)\rangle$ was found by best fitting the outer components of the spectra. The correlation coefficient, R, defined previously (Hustedt et al., 1993), exceeded 0.97 for all spectra reported.

RESULTS

The EPR spectra of NT and DPL are shown in Fig. 6. The distance between the outer spectral features is proportional to the quantity $\langle A_{zz}\rangle$. The decrease in the distance between the outer spectral feature in the DPL spectrum with respect to the NT spectrum is indicative of a more flexible sequence undergoing larger mean squared amplitudes of bending (see Eq. 11). These spectra illustrate the range of spectral responses expected when different test sequences are inserted into DNA with a fixed contour length of ~170 Å. If the DPL connection between basepairs 11 and 12 were to act as a universal swivel joint, or in the context of the model $r = 0$ (Eq. 6), then we could predict the dynamics of the 11-mer. A freely jointed hinge uncouples the internal collective modes of the 11-bp segment (containing the probe) from the rest of the DNA. The 11-bp segment then freely rotates as an independent object about the end connected to the remaining 39-bp segment, rather than about the middle, which is basepair 25, of the full DNA. Rotation about the end of the 11-mer is nearly equivalent to a 22-mer rotating freely about its center. Therefore, Fig. 6 compares the EPR spectrum of DPL with that of a 22-bp-long duplex DNA (NT-22), also labeled at position 6. The high degree of overlap between these two spectra supports the hypothesis that the DPL linker acts nearly as a universal hinge. Others have observed that freely jointed segments increase flexibility in DNA. A single-stranded region of six bases will produce a result nearly equivalent to that of the DPL linker (Reese, 1996). In cyclization assays, Crothers and co-workers detected a hinge in duplex DNA composed of three unpaired bases in a row in 182-bp duplex DNA. The r.m.s. libration amplitude due to the hinge was ~66° (corresponding to a local effective persistence length of ~35 Å), as compared to

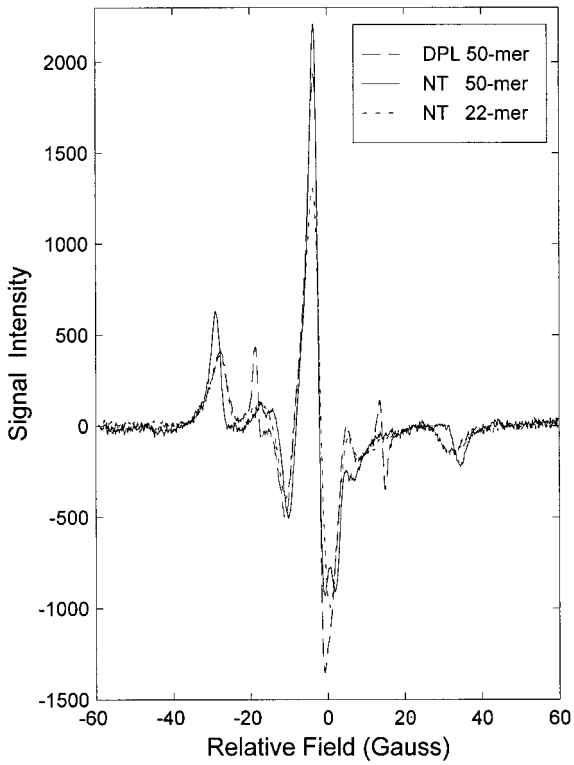

FIGURE 6 The CW-EPR spectra of the 50-mer duplex DNA sequences NT (control) and DPL (NT containing a dipropylene linker between 5′ basepairs 11 and 12) and a 22-mer duplex sequence (NT-22, the first 22 basepairs of the NT sequence). All three sequences are spin labeled with **Q** at position 6 from the 5′ end. Tensors used to simulate the EPR spectra of the [^{14}N,H$_{12}$] isotopic spin label are **A** = 6.58, 4.98, 34.23 Gauss, and **g** = 2.0084, 2.0068, 2.0034 (simulations not shown). The **A** tensors for [^{15}N,D$_{12}$] label are those for [^{14}N,H$_{12}$] divided by 0.733.

the value of a basepair in B-form duplex DNA of ~7° (this corresponds to a persistence length of 500 Å) (Kahn et al., 1994).

$\langle\beta_6^2\rangle$ for the different DNAs listed in Table 1 have been measured. The experimental $\langle\beta_6^2\rangle$ values are plotted against their sequence start positions, N_1, in Fig. 7. The theory (calculated from Eq. 6 for $\langle\beta_6^2\rangle$) is overlaid for the values of L, corresponding to the different lengths of the $(AT)_n$ inserts. Note that all of the curves decay with a correlation length of ~25 bp, as shown in Figs. 4 and 5. A single r of 0.81 ± 0.02 was chosen by a best-fit criterion to simulate the $\langle\beta_6^2\rangle$ data for all of the $(AT)_n$ inserts. A previously determined value of $k_BT/\bar{\kappa}$ was used (Okonogi et al., 1999), but the ratio is insensitive to $\bar{\kappa}$. The r parameter was calculated using dynamic bending persistence lengths ranging from 1200 to 1500 Å and did not vary. A single length-independent $\langle\beta_o^2\rangle$ was added to the theoretical predictions of Eq. 6. $\langle\beta_o^2\rangle$ and r are the only adjustable parameters. The value of $\langle\beta_o^2\rangle$, which was found by a least-squares criterion, was the same, within experimental error, as that measured previously (Okonogi et al., 1999).

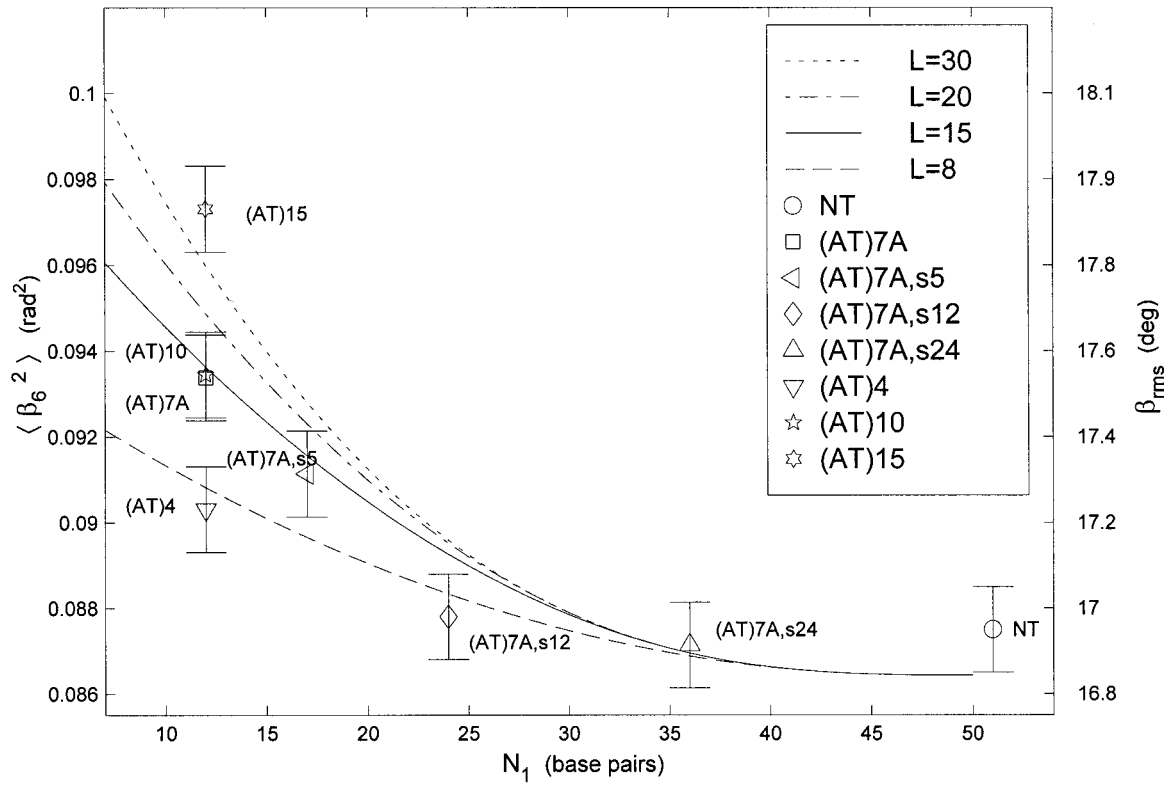

FIGURE 7 $\langle\beta_6^2\rangle$ and β_{rms} values for the sequences given in Table 1. Overlaid is the theory of Eqs. 6 and 7, for $r = 0.81 \pm 0.02$, $k_BT/\bar{\kappa} = 0.00272$ rad^2, which corresponds to a persistence length of 1250 Å at 30°C, and the length independent contribution to $\langle\beta_6^2\rangle$ of $\langle\beta_o^2\rangle = 0.0224 \pm 0.0006$ rad^2. Experimental errors are all less than or equal to ± 0.0015 rad^2.

DISCUSSION

The agreement of the theory with the experiments supports the idea that $(AT)_n$ sequences have a bending force constant that is different from the average basepair and that the effect is local. This is supported by the observation that the $\langle\beta_6^2\rangle$ differences between the control (NT) sequence and the $(AT)_7A$ inserts become smaller as the $(AT)_7A$ inserts are moved farther from the observing spin probe. The effect is not independent of position of the insert relative to the probe. The agreement between the measured values of the amplitude, $\langle\beta_6^2\rangle$, for the inserts, $(AT)_7As_n$, and those computed from the theory (Eqs. 6 and 7) is remarkable in that the fall-off of the effect of the inserts with distance from the probe is not an adjustable parameter of the model. The experiments (shown in Fig. 7) are designed to test both the dependence on L for fixed N_1 and on N_1 for fixed L. There is good agreement, using a single ratio parameter, r, for both sets of experiments. Given the simplicity of the model, which contains only two adjustable parameters, r and the length-independent amplitude, $\langle\beta_o^2\rangle$, the agreement of the calculations with the eight different types of test sequences is excellent. The conclusion that $(AT)_n$ sequences are more flexible than average sequences seems justified.

The correlation length of the effect depends only on the total length of the DNA, regardless of test sequence length or flexibility. The amplitudes of bending are a function of L, N, and r and depend on the position of the test sequence with respect to the probe and the remaining average DNA; but the correlation length is always approximately half the length of the DNA duplex. Small permanent (or static) bends in the DNA do not appreciably reduce the effects of the coupling as seen throughout the molecule (Okonogi et al., 1997). In a much longer filament, this effect must be cut off by the equilibrium total persistence length of the DNA, $P_{tot} = 500$ Å.

The fact that not all of the experimental $\langle\beta_6^2\rangle$ values (including their errors) in Fig. 7 lie on the calculated decay curves is due in part to the simplicity of the model. The experiments presented herein do not allow a distinction between (AT) and (TA) steps, and the flexibility, parameterized by r, must be considered a weighted average of the (AT) and (TA) step flexibilities. Should (AT) and (TA) steps have different flexibilities, the relative flexibility ratios can be defined as $r_{(AT)}$ and $r_{(TA)}$. The ratio parameter we report, $\bar{r}$, is the average of these two ratios, given by $1/\bar{r} = 0.52\ (1/r_{(AT)}) + 0.48(1/r_{(TA)})$. This average was determined using Eqs. 6 and 7 modified to accept two different ratio parameters. More extensive experiments and analysis that allow for distinctions between basepairs (Okonogi et al., 1997, 1998) will be published elsewhere.

Moreover, the motion may be highly anisotropic, and the value reported here represents an average bending amplitude and force constant.

It is not surprising that we find $(AT)_n$ sequences more flexible than average. Others have observed qualitative differences in binding and have attributed the differences to increased local flexibility in duplex DNA associated with (AT)-rich sequences or regions. For example, any of a number of permutations of an (AT)-rich sequence, next to the GC box that binds the MIG1 zinc finger protein, was found to be essential for high-affinity binding, even though no single base within this region was conserved (Lundin et al., 1994). Lundin et al. (1994) concluded that "MIG1 recognizes the AT box directly, but in a way that requires bendable DNA rather than a unique sequence motif." It is now possible to assign a magnitude to the increased bending made possible by the presence of $(AT)_n$ steps.

The bending in $(AT)_n$ sequences increases by 10% for the same amount of energy, and 20% less energy is required for the same amount of bending, because the bending constant for $(AT)_n$ is 0.8 times that for average DNA and because $\langle \Delta\beta_i^2(\infty) \rangle = 2(kT/\kappa_i)$. At room temperature, the average bending between base pairs is $\sim 3°$, and a 20% increase in flexibility increases the mean relative bending angle to $\sim 3.5°$. The associated radius of curvature, then, decreases from 65 Å to 56 Å with a 0.5° increase in the mean bending angle, moving the radius of curvature significantly closer to the 45-Å radius necessary for histone formation.

This measured value of 0.8 may be compared with that of Hogan and Austin, who found the dynamic torsional and flexural rigidities of AT basepairs to be 0.5 times that for an average DNA. Their experiments differed from those presented here in that Hogan and Austin studied only homopolymers and heteropolymers and based their conclusions on percentage base pair composition and not sequence. In contrast to the findings of Hogan and Austin, Fujimoto and Schurr (1990) found virtually no variation in the torsional rigidity with base composition for 0–66% AT, and we find a substantially smaller variation of the flexural rigidity with composition than that suggested by Hogan and Austin. Nevertheless, when the induced bend is sufficiently great, this component of the total flexural rigidity makes a significant contribution to the differences in the binding energy of $(AT)_n$-containing sequences.

Nucleosomal reconstitution experiments have provided qualitative but inconclusive evidence that $(AT)_n$ steps are more flexible than $(AA)_n$ steps (Hagerman, 1988). More recent work suggests that DNA packaging around the histones involves a cooperative effect between static bends and flexible sequences, and properly phased AAA sequences may orient the DNA minor groove to the protein surface, while AT repeats provide the local flexibility needed to accommodate the necessary radius of curvature of 45 Å (Drew and Travers, 1985; Satchwell et al., 1986). The TATA-box binding protein, TBP, induces a 90° bend in duplex DNA at the TATA binding region, employing the TA steps and TAAA sequence. The large bend angles are very likely a combination of a greater than normal flexing ability, phenylalanine residue insertion, and unwinding of the box toward the underside of the protein (Patikoglou and Burley, 1997). In addition to the structural motifs of TBP binding, there is thought to be an additional contribution due to increased flexibility of the resulting protein-DNA complex. Thus the sequence-dependent flexibilities may also play a significant part in the overall energetics of DNA-protein recognition (Patikoglou and Burley, 1997).

We find that DPL inserts that are 2 bp in length and single-strand bases are extremely flexible motifs and are far more flexible than any duplex basepair step. This correlates well with the results of Kahn et al. (1994), who used strings of three unpaired bases (or loops) to induce local flexibility. Grove et al. have used regions of two unpaired bases consisting of 4Ts (called 4nT loops) to enhance the binding of TF1 (Grove et al., 1996b) and IHF and HMG1 (Grove et al., 1996a) to their respective DNAs. These binding experiments tested the idea that DNA bending proteins may depend on sequence-dependent flexibility of the DNA operator. The binding experiments showed a high degree of correlation between the predictions of sequence-dependent flexure, which assumed flexibility of the 4nT loops and the observed enhanced binding. They (Grove et al., 1996a,b) concluded that local DNA flexibility and not sequence played a central role in recognition of the DNA by DNA bending proteins. They also demonstrated that the context of the position of the flexible 4nT loops was very important and that sequence-dependent flexure is tied to context. Therefore, a quantitative assessment of the extent of sequence-dependent flexure would contribute to a clearer understanding of the binding energetics of DNA by bending proteins.

The decrease of an effect with length of DNA has been observed in another experiment. The process of insert deletion in *B. subtilis* has been studied. Inserts are determined by the presence of tandem 18-bp directed repeats, which flank the insert. The sequence that intervenes between the tandem repeats is deleted. The rate at which the inserts are removed has been studied as a function of insert length. It was found that the rate decreased exponentially with increasing insert length for insert lengths in excess of 300 bp. The correlation length is around 500 Å. This process was explained in terms of internal DNA flexibility (Chedin et al., 1994). This result exemplifies how flexibility can control a biological process: When the rate-limiting step is diffusion-controlled, it is possible for enhanced flexibility at one site to affect the kinetics of a process taking place at another, distant site. In general, long-range dynamical correlations have no effect on the kinetics or equilibria processes controlled by a transition state when those properties are determined by equilibrium statistical mechanics, except

when an enhanced flexibility allows new tertiary contacts within the molecule.

CONCLUSIONS

DNA binding proteins for non-sequence-specific binding may partially depend on the sequence's ability to bend or flex. Increased flexibility in a region means that $\langle \Delta\beta_i^2(\infty)\rangle$, or the mean squared flexing angle between neighboring basepairs, increases from an average value. The sequence dependence of the bending rigidity may provide a basis of discrimination for protein binding to the extent that local bendability is sequence dependent and contributes to the binding energetics. Regions of DNA communicate dynamically with other regions of DNA through the internal normal modes. The magnitude of the internal librations, $\langle \beta_i^2(\infty)\rangle$, can be augmented with additional DNA, while $\langle \Delta\beta_i^2(\infty)\rangle$ cannot. Dynamical communication along the molecule, as measured by $\langle \beta_i^2(\infty)\rangle$, decays with a correlation length around half the length of the DNA molecule, up to a persistence length.

The experiments presented herein constitute the first quantitative demonstration of the existence of site-specific sequence-dependent flexibility of duplex DNA. This type of experiment clearly distinguishes between dynamic bending and static or permanent bends. The development of this model to describe the relative flexibility of dinucleotide steps suggests that each of the distinct nucleotide steps can ultimately be parameterized by a series of force constants, and that the flexibility of $(AT)_n$ basepair steps is 0.8 times the flexibility of average basepairs. With such a set of parameters in hand, the contribution of sequence-dependent duplex DNA flexibility to biological processes, such as protein recognition and chromatin packaging, can be addressed.

Thanks to J. M. Schurr for a careful reading of the manuscript and many helpful suggestions.

This work was supported in parts by grants from the National Institute of Health (GM 32681, GM 55963, and GM 08268 to AWR) and NIEHS Environmental Sciences Center grant P30 ESO7033, as well as a fellowship from the American Chemical Society (to SCA).

REFERENCES

Allison, S. A., J. H. Shibata, J. Wilcoxon, and J. M. Schurr. 1982. NMR relaxation in DNA. I. The contribution of torsional deformation modes of the elastic filament. *Biopolymers.* 21:729–762.

Aloyo, M. C., D. Campbell, N. J. Combates, J. Gonzales, Y. Kwok, R. D. Sheardy, and S. A. Winkle. 1993. Restriction enzymes have altered cleavage rates at sites near certain sequences. *Biophys. J.* 64:A280.

Chedin, F., E. Dervyn, R. Dervyn, S. D. Ehrlich, and P. Noirot. 1994. Frequency of deletion formation decreases exponentially with distance between short direct repeats. *Mol. Microbiol.* 12:561–569.

Dlakic, M., and R. E. Harrington. 1995. Bending and torsional flexibility of G/C-rich sequences as determined by cyclization assays. *J. Biol. Chem.* 270:29945–29952.

Drew, H. R., and A. A. Travers. 1985. DNA bending and its relation to nucleosome positioning. *J. Mol. Biol.* 186:773–790.

Fujimoto, B. S., and J. M. Schurr. 1990. Dependence of the torsional rigidity of DNA on base composition. *Nature.* 344:175–177.

Grove, A., A. Galeone, L. Mayol, and E. P. Geiduschek. 1996a. Localized DNA flexibility contributes to target site selection by DNA-bending proteins. *J. Mol. Biol.* 260:120–125.

Grove, A., A. Galeone, L. Mayol, and E. P. Geiduschek. 1996b. On the connection between inherent DNA flexure and preferred binding of hydroxymethyluracil-containing DNA by the type II DNA-binding protein TF1. *J. Mol. Biol.* 260:196–206.

Hagerman, P. J. 1988. Flexibility of DNA. *Annu. Rev. Biophys. Biophys. Chem.* 17:265–286.

Hagerman, P. J. 1990. Sequence directed curvature of DNA. *In* Annual Review of Biochemistry. D. M. Engelman, C. R. Cantor, and T. D. Pollard, editors. Annual Reviews, Palo Alto, CA. 755–781.

Harrington, R. E., and I. Winicov. 1994. New concepts in protein-DNA recognition: sequence-directed DNA bending and flexibility. *Prog. Nucleic Acid Res. Mol. Biol.* 47:195–270.

Hogan, M. E., and R. H. Austin. 1987. Importance of DNA stiffness in protein-DNA binding specificity. *Nature.* 329:263–266.

Hustedt, E. J., A. Spaltenstein, J. J. Kirchner, P. B. Hopkins, and B. H. Robinson. 1993. Motions of short DNA duplexes: an analysis of DNA dynamics using an EPR-active probe. *Biochemistry.* 32:1774–1787.

Kahn, J. D., E. Yun, and D. M. Crothers. 1994. Detection of localized DNA flexibility. *Nature.* 368:163–166.

Kim, U. S., B. S. Fujimoto, C. E. Furlong, J. A. Sundstrom, R. Humbert, D. C. Teller, and J. M. Schurr. 1993. Dynamics and structures of DNA: long-range effects of a 16 base-pair (CG)8 sequence on secondary structure. *Biopolymers.* 33:1725–1745.

Lundin, M., J. O. Niehlin, and H. Ronne. 1994. Importance of a flanking AT-rich region in target site recognition by the GC box-binding zinc finger protein MIG1. *Mol. Cell. Biol.* 14:1979–1985.

Mailer, C., D. A. Haas, E. J. Hustedt, J. G. Gladden, and B. H. Robinson. 1991. Low-power electron paramagnetic resonance spin-echo spectroscopy. *J. Magn. Res.* 91:475–496.

Maniatis, T., E. F. Fritsch, and J. Sambrook. 1989. Molecular Cloning: A Laboratory Manual. Cold Spring Harbor Laboratory, Cold Spring Harbor, NY.

Miller, T. R., S. C. Alley, A. W. Reese, M. S. Solomon, W. V. McCallister, C. Mailer, B. H. Robinson, and P. B. Hopkins. 1995. A probe for sequence-dependent nucleic acid dynamics. *J. Am. Chem. Soc.* 117: 9377–9378.

Naimushin, A., B. S. Fujimoto, and J. M. Schurr. 2000. Dynamic bending rigidity of a 200 bp DNA in 4 mM ionic strength: a transient polarization grating study. *Biophys. J.* 78:1498–1518.

Nardulli, A. M., L. E. Romine, C. Carpo, G. L. Greene, and B. Rainish. 1996. Estrogen receptor affinity and location of consensus and imperfect estrogen response elements influence transcription activation of simplified promoters. *Mol. Endocrinol.* 10:694–704.

Okonogi, T. M., A. W. Reese, S. C. Alley, P. B. Hopkins, and B. H. Robinson. 1997. Sequence dependent dynamics of duplex DNA. *In* 20th International EPR Conference, 39th Rocky Mountain Conference, Denver, CO (poster).

Okonogi, T. M., A. W. Reese, S. C. Alley, P. B. Hopkins, and B. H. Robinson. 1998. How far does bending flexibility transmit in duplex DNA? *Biophys. J.* 72:A287 (poster).

Okonogi, T. M., A. W. Reese, S. C. Alley, P. B. Hopkins, and B. H. Robinson. 1999. Flexibility of duplex DNA on the sub-microsecond timescale. *Biophys. J.* 77:3256–3276.

Patikoglou, G., and S. K. Burley. 1997. Eukaryotic transcription factor-DNA complexes. *In* Annual Review of Biophysics and Biomolecular Structure. W. L. H. R. M. Stroud, W. K. Olson, M. P. Sheetz, editors. Annual Reviews, Palo Alto, CA. 289–325.

Ramsauer, V., L. Aguilar, M. Ballester, R. D. Sheardy, and S. A. Winkle. 1997. The conformation of (CG) DNA segments regulates RNA polymerase activity. *Biophys. J.* 72:A98.

Reese, A. W. 1996. Analysis of CW-EPR spectra and the internal dynamics of DNA. Ph.D. thesis. University of Washington, Seattle, WA.

Richmond, T. J., J. T. Finch, B. Rushton, D. Rhodes, and A. Klug. 1984. Structure of the nucleosome core particle at 7 Å resolution. *Nature.* 311:532–537.

Satchwell, S. C., H. R. Drew, and A. A. Travers. 1986. Sequence periodicities in chicken nucleosome core DNA. *J. Mol. Biol.* 191:659–675.

Schellman, J. A., and S. C. Harvey. 1995. Static contributions to the persistence length of DNA and dynamic contributions to DNA curvature. *Biophys. Chem.* 55:95–114.

Schurr, J. M., J. J. Delrow, B. S. Fujimoto, and A. S. Benight. 1997a. The question of long-range allosteric transitions in DNA. *Biopolymers.* 44: 283–308.

Schurr, J. M., B. S. Fujimoto, and B. H. Robinson. 1997b. Diffusional spinning as a probe of DNA fragment's conformation (comment). *J. Chem. Phys.* 106:815–816.

Schurr, J. M., U. S. Kim, L. Song, and B. S. Fujimoto. 1991. Dynamics and structures of DNA. *Biochem. Soc. Trans.* 19:497.

Song, L., and J. M. Schurr. 1990. Dynamic bending rigidity of DNA. *Biopolymers.* 30:229–237.

Thompson, B. J., M. N. Camien, and R. C. Warner. 1976. Kinetics of branch migration in double-stranded DNA. *Proc. Natl. Acad. Sci. USA.* 73:2299–2303.

Wolffe, A. P. 1994. Architectural transcription factors (comment). *Science.* 264:1100–1101.

Wu, P., B. S. Fujimoto, and J. M. Schurr. 1987. Time-resolved fluorescence polarization anisotropy of short restriction fragments: the friction factor for rotation of DNA about its symmetry axis. *Biopolymers.* 26:1463–1488.